Atmos. Chem. Phys. Discuss., 12, 21321–21353, 2012
www.atmos-chem-phys-discuss.net/12/21321/2012/
doi:10.5194/acpd-12-21321-2012

Atmospheric Chemistry and Physics Discussions

Immersion freezing of ice nucleating active protein complexes

S. Hartmann, S. Augustin, T. Clauss, J. Voigtländer, D. Niedermeier, H. Wex, and F. Stratmann

Leibniz Institute for Tropospheric Research, Permoserstr. 15, 04318 Leipzig, Germany

Received: 25 July 2012 – Accepted: 13 August 2012 – Published: 21 August 2012

Correspondence to: S. Hartmann (hartmann@tropos.de)

Published by Copernicus Publications on behalf of the European Geosciences Union.

Abstract

Biological particles, e.g. bacteria and their Ice Nucleating Active (INA) protein complexes, might play an important role for the ice formation in atmospheric mixed-phase clouds. Therefore, the immersion freezing behavior of INA protein complexes generated from a Snomax^{TM} solution/suspension was investigated as function of temperature in a range of −5 °C to −38 °C at the Leipzig Aerosol Cloud Interaction Simulator (LACIS). The immersion freezing of droplets containing small numbers of INA protein complexes occurs in a temperature range of −7 °C and −10 °C. The experiments performed in the lower temperature range, where all droplets freeze which contain at least one INA protein complex, are used to determine the average number of INA protein complexes present, assuming that the INA protein complexes are Poisson distributed over the droplet ensemble. Knowing the average number of INA protein complexes, the heterogeneous ice nucleation rate and rate coefficient of a single INA protein complex is determined by using the newly-developed CHESS model (stoCHastic model of idEntical poiSSon distributed ice nuclei). Therefore, we assume the ice nucleation process to be of stochastic nature, and a parameterization of the INA protein complex's nucleation rate. Analyzing the results of immersion freezing experiments from literature (Snomax^{TM} and *Pseudomonas syringae* bacteria), to results gained in this study, demonstrates that first, a similar temperature dependence of the heterogeneous ice nucleation rate for a single INA protein complex was found in all experiments, second, the shift of the ice fraction curves to higher temperatures can be explained consistently by a higher average number of INA protein complexes being present in the droplet ensemble, and finally the heterogeneous ice nucleation rate of one single INA protein complex might be also applicable for intact *Pseudomonas syringae* bacteria cells. The results obtained in this study allow a new perspective on the interpretation of immersion freezing experiments considering INA protein complexes and the derived simple parameterization of the heterogeneous ice nucleation rate can be used in cloud resolving models for studying the effect of bacteria induced ice nucleation.

ACPD

12, 21321–21353, 2012

1 Introduction

Atmospheric observations indicate that heterogeneous ice nucleation in mixed-phase clouds can already occur at temperatures higher than −20 °C (Ansmann et al., 2009; Seifert et al., 2010). In contrast, laboratory studies showed that the majority of components found in atmospheric ice crystal residues are only ice active at lower temperatures. Natural mineral dust and soot belong to these major constituents of ice crystal residues (e.g. Pratt et al., 2009; Kamphus et al., 2010; Twohy and Poellot, 2005). One possible explanation for the observed temperature differences might be the presence of biological particles (e.g. bacteria) acting as Ice Nuclei (IN) already at temperatures above −10 °C. Ice Nucleating Active (INA) bacteria, being ubiquitous in the atmosphere, are currently the most efficient IN known (e.g. Möhler et al., 2008; Yankofsky et al., 1981; Levin and Yankofsky, 1983; Vali et al., 1976). Investigating the freezing behavior of one of these INA bacteria, in particular *Pseudomonas syringae*, Maki et al. (1974) found freezing temperatures of about −2 °C. INA bacteria strains possess special protein complexes anchored in the outer bacterial membrane able to mimic the structure of ice (Warren and Wolber, 1987; Ward and DeMott, 1989; Wolber and Warren, 1989). These ice nucleating active protein complexes act as a template for ice cluster formation by reducing the energy barrier required for critical ice cluster formation. Due to chemical heterogeneity or different chemical structures, the ice nucleation potential, manifesting itself in e.g. different threshold temperatures for ice nucleation, which can vary between INA protein complexes (e.g. Wolber and Warren, 1989; Southworth et al., 1988). Thereby, size (e.g. available OH-groups), structural fidelity (lattice match) and attached non-protein membrane components might matter for the ice nucleation efficiency of the INA protein complexes.

The INA protein structures are divided into three major classes (Turner et al., 1991) related to freezing temperature range. According to Turner et al. (1990, 1991) and Cochet and Widehem (2000), class A protein structures exist very rarely (approximately 1 out of 10^4 bacteria possess such an protein complex) and initiate freezing at

ACPD
12, 21321–21353, 2012

$T > -4.4\,^{\circ}C$. Class B protein structures are ice active in a range of $-4.8 \leq T \leq -5.7\,^{\circ}C$ and are more abundant. Class C protein structures are found on almost all INA bacteria cells with a threshold freezing temperature below $-7.6\,^{\circ}C$.

In general, since the seventies of the last century many studies investigating the ice nucleation behavior of bacteria have been performed (e.g. Maki et al., 1974; Turner et al., 1990; Cochet and Widehem, 2000; Vali et al., 1976; Yankofsky et al., 1981; Maki and Willoughby, 1978; Lindow et al., 1982; Levin and Yankofsky, 1983). In most of these studies, the freezing of droplets with multiple (10^3 to 10^8) immersed bacteria cells per droplet was analyzed and freezing temperature values were determined. However, to understand the heterogeneous ice nucleation behavior of the bacterial INA protein complexes more precisely, it is necessary to analyze the freezing of droplets which contain only a small and defined number of bacteria cells and/or INA protein complexes. Such a scenario is also much closer to atmospheric conditions under which more than one IN per droplet, and consequently a large number of INA protein complexes per droplet is rather unlikely.

The ice nucleation behavior of air-suspended bacteria or bacteria related particles (e.g. Snomax^{TM}) was investigated by Möhler et al. (2008) and Wood et al. (2002). However, these investigations were performed for polydisperse IN distributions which makes interpretation and quantification of specific properties of the INA protein structures difficult. Furthermore, considering the stochastic nature of the heterogeneous ice nucleation process while trying to quantify the ice nucleation behavior of INA protein structures, instead of threshold temperatures, nucleation rates and/or nucleation rate coefficients need to be determined as a function of temperature. Investigations comprising both, a small number of INA protein complexes per droplet and the determination of nucleation rates and/or nucleation rate coefficients do not exist up to now. Therefore, we investigated the immersion freezing behavior of air-suspended droplets, each containing a well-defined number of INA protein complexes, generated from a Snomax^{TM} suspension/solution, functioning as model substance for *Pseudomonas syringae* bacteria.

ACPD
12, 21321–21353, 2012

The investigations were performed at the Leipzig Aerosol Cloud Interaction Simulator (LACIS; Stratmann et al., 2004; Hartmann et al., 2011).

In the following, the results gained concerning the number of INA protein complexes per droplet and the nucleation rate/rate coefficient for one of the INA protein complexes controlling the ice nucleation ability of Snomax^{TM} will be presented. Therefore, the newly developed classic nucleation theory based nucleation model CHESS (stoCHastic model of idEntical ice nuclei poiSSon distributed) was applied.

2 Theory

In Niedermeier et al. (2011a), it is shown that the fundamental nature of heterogeneous ice nucleation is stochastic. Therefore, in the present paper, we quantify heterogenous ice nucleation (here specifically immersion freezing) in terms of the ice nucleation rate coefficient j_{het}, which has the unit #/m^2 s and depends on temperature T. Considering a supercooled droplet population (total number N_0) at a constant temperature, with the IN immersed in the droplets having identical ice nucleation properties, i.e, nucleation rate coefficients j_{het}, the time rate of change for the number of unfrozen droplets N_u is given by (e.g. in Pruppacher and Klett, 1997):

$$\frac{dN_u}{dt} = -N_u S_{site} j_{het}(T). \quad (1)$$

Here S_{site} is the surface area of the ice nucleating site. Integrating Eq. (1) for a constant temperature T over time t, the fraction of frozen droplets f_{ice} (number of frozen droplets, N_f, divided by the total number of droplets $N_0 = N_f + N_u$) can be calculated as

$$f_{ice}(T) = 1 - \frac{N_u}{N_0}(T) = \frac{N_f}{N_0}(T) = 1 - \exp(S_{site} j_{het}(T) t). \quad (2)$$

ACPD
12, 21321–21353, 2012

3 Material and measurement method

3.1 Material–Snomax™

Snomax™ (Johnson Controls Snow, Colorado, USA) consists of deadened *Pseudomonas syringae* bacteria, fragments of those, several proteins, carbohydrates and remnants of the nutrition medium used for bacteria cultivation. Usually, Snomax™ is utilized for artificial snow production. The *Pseudomonas syringae* bacteria used in Snomax™ production are grown under ideal conditions to maximize their IN ability. Hence Snomax™ has a bacterial origin, it is considered as a convenient model substance for highly ice nucleation active bacteria.

3.2 LACIS

LACIS allows for the investigation of the immersion freezing behavior of well-characterized, size-selected particles as function of temperature with only one particle being immersed in each droplet. In this section, the setup and operating principle will be described briefly, especially with respect to technical innovations, compared to former experiments as described in Stratmann et al. (2004); Niedermeier et al. (2010, 2011b) and Hartmann et al. (2011).

The schematic setup of the particle generation, the LACIS flow tube and the optical detection system are shown in Fig. 1. For producing aerosol particles, 1.6 g Snomax™ pellets were dissolved/suspended in 1 l double deionized water. The solution/suspensions was atomized (atomizer: TSI 3075, TSI Inc., St. Paul, Minnesota, USA) and the resulting aerosol was dried in a diffusion dryer. Subsequently, the resulting dry particles were size selected using a Differential Mobility Analyzer (DMA, Knutson and Whitby (1975), type "Vienna medium"), and then fed into LACIS.

A particle free sheath air flow was conditioned with respect to humidity by mixing a dry and a defined humidified (humidifier, PH-30T-24KS, Perma Pur, Toms River, New Jersey) air flow prior to entering the flow tube. A chilled mirror dew point hygrometer

ACPD
12, 21321–21353, 2012

(DPM, DPM 973, MBW Calibration Ltd., Wettingen, Switzerland) was used to monitor the dew point of the sheath air flow. The aerosol and sheath air flows were combined in the inlet section of LACIS, which serves as heat exchanger for harmonizing the inlet temperatures of both air flows. The sheath air enters the laminar flow tube isokinetically with the aerosol flow, with the latter forming an approximately 2-mm-diameter aerosol beam at the center of the flow tube. LACIS itself consists of seven connected one-meter tube sections with an inner diameter of 15 mm. The wall temperature of each tube section is set separately by different thermostats (TH).

At the outlet of LACIS, the Thermally Stabilized Optical Particle Spectrometer (TOPS-ICE, developed and built at IfT, Clauss et al., 2012) is used to determine both, the number and the phase state of the hydrometeors. The phase state distinction takes place via the evaluation of the polarization state of scattered light in 42.5° forward direction. By means of TOPS-ICE the ice fraction and the size of the droplets and ice particles can be analyzed.

Investigating the immersion freezing behavior of biological particles the temperature range of LACIS was extended to higher temperatures ranging from 0 to −25 °C. This is an innovation compared to older studies (Niedermeier et al., 2010, 2011b; Hartmann et al., 2011) in which the temperature range of −26 °C to −40 °C was covered. Furthermore, in contrast to former investigations, LACIS was run such that both droplets and ice particles were present at the outlet of LACIS. The utilization of the newly-developed TOPS-ICE instrument Clauss et al. (2012) allowed the determination of the ice fraction when both, droplets and ice particles, are present.

The following LACIS parameters were used for the experiments performed at higher temperature range: the inlet as well as the wall temperature of sections 1 to 5 were set to 25.0 °C, the inlet dew point temperature was varied in a range from 23.7 °C to 24.2 °C. The inner tube wall of section 6 was covered with liquid water having a temperature of 0 °C. The wall temperature of section 7 was set to the respective temperature of interest ranging from 0 °C to −25 °C with the inner tube wall being covered with ice.

ACPD
12, 21321–21353, 2012

In Fig. 2 modeled (combined FLUENT/FPM; FLUENT: ANSYS Inc., Canonsburg, PA, USA; FPM: Particle Dynamics GmbH, Leipzig, Germany, Wilck et al., 2002) temperature (upper panel) and saturation wrt. water and ice (lower panel) at the centerline of sections 6 and 7 are depicted exemplarily for wall temperatures of −5 °C, −10 °C and −15 °C.

The temperature profiles show a steep decrease in section 6 and approach the externally-set wall temperatures of 0 °C at the end of the section. Due to the lower wall temperature in section 7 the temperature decreases further. At the end of section 7 the temperature at the centerline matches the set wall temperatures with a deviation of 0.30 K for −5.00 °C, of 0.53 K for −10.00 °C and of 0.76 K – 15.00 °C wall temperature setting. These temperature deviations are accounted for in the data evaluation. In other words, results are reported in terms of center line temperatures.

As can be seen in the lower panel of Fig. 2, the saturation wrt. water rises very steeply in section 6, reaches its maximum and decreases again approaching water saturation at the end of section 6. As soon as the critical super-saturation is reached, the particles are activated to droplets and these droplets grow dynamically, depending on the prevailing saturation, to sizes of about 4 µm at the end of section 6. The water saturation decreases further in case of −5 °C wall temperature. For wall temperatures of −10 °C and −15 °C, the saturation wrt. water increases again at the beginning of section 7. This leads to further droplet growth. For all settings the water-saturation then falls below 1, while the saturation wrt. ice approaches 1. Consequently, droplets evaporate slightly in the prevailing ice super-saturated and water sub-saturated environment. All experiments were carried out for similar droplet sizes at the end of section 7. Therefore, the inlet dew point temperature, as second parameter for controlling droplet size was adjusted accordingly. Droplets at the outlet of LACIS featured sizes of 2.5 ± 0.5 µm.

In addition to the measurements performed in the temperature range between 0 °C to −25 °C, experiments were also carried out at lower temperatures (ranging from −26 °C to −40 °C), following the operation mode described in Hartmann et al. (2011), however,

ACPD
12, 21321–21353, 2012

with higher inlet dew point temperatures to ensure that both droplets and ice particles pass through the outlet of LACIS.

4 Results and discussion

4.1 Experimental results

The immersion freezing behavior of size-selected particles (mobility diameter D_P: 100, 300, 400, 650 and 800 nm) generated from a Snomax^{TM} suspension/solution was studied. Especially for 650 nm and 800 nm particles, the ice fraction f_{ice} was analyzed as function of temperature in the range from −5 °C to −38 °C. The results are shown in Fig. 3. The ice fraction curves are very steep, almost linear for temperature values between −7 °C and −10 °C. The respective measurement uncertainties are represented by single standard deviations determined from at least 3 independent measurements performed under identical conditions.

As can be seen, for $T \leq -15$ °C, the ice fraction curves level off to constant values of about 0.2 and 0.4 for the 650 and 800 nm particles, respectively. As the ice fractions do not increase any further, we conclude that a saturation regime is reached, i.e. there are no further IN which can initiate freezing at lower temperature. This suggests that only 20 % of 650 nm and 40 % of 800 nm particles generated from Snomax^{TM} solution/suspension are ice active. As it is fact that INA protein complexes are constituents of Snomax^{TM} and initiate heterogeneous ice nucleation, this implies that only 20 % of 650 nm and 40 % of 800 nm particles generated from Snomax^{TM} solution/suspension contain one or more INA protein complexes, or in other words, the unfrozen droplets do not even contain a single INA protein complex.

Before looking into that in more detail, it should be clarified which INA protein complexes contained in Snomax^{TM} are present in the droplets investigated. According to Turner et al. (1990, 1991) three different classes, A, B, and C of such protein complexes exist, defined via the temperature at which ice nucleation is initiated: $T < -4.4$ °C,

ACPD
12, 21321–21353, 2012

$-4.8 \leq T \leq -5.7\,^{\circ}\mathrm{C}$ and $T < -7.6\,^{\circ}\mathrm{C}$, for classes A, B, and C, respectively. Since the slope of the logarithm of f_{ice} increases linearly in the temperature range from $-7\,^{\circ}\mathrm{C}$ to $-10\,^{\circ}\mathrm{C}$, we conclude that only one class of INA protein complexes is present in the droplets. To strictly identify which specific class of INA protein structures is present in the droplets investigated is difficult. However, we can speculate which of them is most likely. For the performed experiments, only a very small amount of protein complexes (particles in a size range of 100 to 800 nm) is present in a droplet. 1000 to 10 000 frozen droplets containing INA protein complexes were counted for determining the ice fractions. Considering the probabilities given in the introduction, it is unlikely, that class A and B proteins are present in the droplets in detectable amounts. This, together with the fact that we observe a strong increase in the ice fraction in a temperature range similar to that reported by Turner et al. (1990) for class C INA protein structures, is suggestive for class C protein structures being the dominating INA protein structures in our experiments.

Having identified the type of INA protein complex most likely inducing droplet freezing in the present experiments, we return to the ice fractions, their saturation behavior, and the resulting consequences. The left panel of Fig. 4 shows ice fractions in the saturation range, denoted as $f^{\star}_{\mathrm{ice}}$, measured at $-15\,^{\circ}\mathrm{C}$ as function of particle size. For 100 nm particles, we observed almost no freezing. In general, $f^{\star}_{\mathrm{ice}}$, and consequently the number of INA protein complexes present in the particles increases with increasing mobility diameter D_{P}, but not in a linear manner.

The facts that (i) not all droplets contain an INA protein complex initiating freezing, (ii) we are able to identify nucleation events induced by single protein complexes, and (iii) that the number of protein complexes present in a droplet is related to particle size offers several possibilities. Specifically these are: (a) the determination of the average number of INA protein complexes distributed over the droplet ensemble (b) the determination of the IN size distribution underlaying the particle size distribution resulting from atomization of the Snomax$^{\mathrm{TM}}$ suspension/solution (c) the determination of the nucle-

ACPD
12, 21321–21353, 2012

ation rate/rate coefficient for a single INA protein complex as function of temperature. These topics will be dealt with in the following.

4.2 Poisson distribution of identical IN

Since not all droplets contain an INA protein complex and the number of INA protein complexes vary between particles generated from a Snomax^{TM} suspension/solution, we consider the number of INA protein structures to be Poisson distributed over the monodisperse particle population (a similar approach can be found in Vali (1971) and Yankofsky et al. (1981)) with parameter λ and number of INA protein complexes, the random number X, varying in a range of $k = 0, \ldots, n$:

$$P_\lambda(X = k) = \frac{\lambda^k}{k!} \exp(-\lambda). \quad (3)$$

The measured ice fraction f_{ice}, and consequently also f^*_{ice}, correspond to a probability of freezing. A droplet can only freeze if it contains at least one INA protein complex. Therefore, the probability that a particle generated from a Snomax^{TM} solution/suspension of a certain size does not contain an INA protein complex can be written as

$$P(X = 0) = \exp(-\lambda) = 1 - f^*_{ice} \quad (4)$$

and consequently,

$$\lambda = -\ln(1 - f^*_{ice}). \quad (5)$$

The parameter λ then describes the expected number of INA protein complexes per particle/droplet. Equation (5) is defined only for $f^*_{ice} < 1$, i.e., in other cases λ cannot be determined. Resulting λ values are given in the right panel of Fig. 4 in relation to particle volume. As can be seen, λ is a linear function of D_P^3 illustrated by the linear fit (red line). This dependence of λ on particle volume can be explained by the fact that,

ACPD
12, 21321–21353, 2012

the larger the particle generated from the Snomax^{TM} suspension/solution, the higher is the amount of dissolved/suspended material contained in it and, hence, the higher is the probability for the presence of one or more INA protein complexes.

Knowing λ as function of particle volume (illustrated in Fig. 4 (right panel)), the probability distribution of INA protein complexes can be calculated by the means of Eq. (3), see Fig. (5). Considering a population of 100 nm particles, the majority of particles contain no INA protein complex ($k = 0$) and only a very small fraction of 10^{-3} include one protein complex ($k = 1$). For 300 nm particles, the fraction of particles containing one INA protein complex is higher and, furthermore, a minor fraction of droplets have two INA protein complexes. For a diameter of 800 nm 40 % of all particles contain either 1, 2, 3, 4 or 5 INA protein complexes.

The IN number size distribution n_{IN} can be determined from the number size distribution of the particles generated from the Snomax^{TM} suspension/solution n_0:

$$n_{IN} = [1 - \exp(-\lambda(D_P^3))]n_0. \quad (6)$$

and is illustrated in Fig. 6. This Figure shows clearly that the majority of the particles do not contain an INA protein complex and, therefore, do not function as an ice nucleus, whereby the ratio of IN to non-IN increases with increasing particle diameter. This is in contradiction to Möhler et al. (2008) who speculated, based on polydisperse measurements, that only particles in the larger mode ($D_P \geq 600$ nm) of the bimodal size distribution are ice active. Indeed, results obtained in the study of Wood et al. (2002) support the assumption that INA protein complexes exist also in smaller size classes, because they analyzed fragments of a Snomax^{TM} solution/suspension smaller than 200 nm and observed immersion freezing.

Knowing the IN size distribution, the expected ice fraction from a polydisperse immersion freezing experiment can be derived by dividing the integral over the IN size distribution by the integral over the particle size distribution. For the distributions shown in Fig. 6 we calculate an expected ice fraction of 0.4 % at $T = -15\,^{\circ}C$. This agrees well with the result of a polydisperse measurement performed at LACIS at $T = -15\,^{\circ}C$, re-

ACPD
12, 21321–21353, 2012

sulting in an ice fraction of 0.55 %. The slightly higher experimentally determined value can be explained by the fact that for the prediction only particle sizes up to 800 nm were considered and it is likely that some particles generated from a Snomax^{TM} suspension/solution larger 800 nm (probably up to about 1300 nm) containing INA protein complexes do exist.

4.3 The CHESS model

Knowing the number of INA protein complexes per particle/droplet, we now can derive the heterogeneous ice nucleation rate/rate coefficient for a single INA protein complex. Therefore, combining the assumptions that (a) heterogeneous ice nucleation is a stochastic process (Niedermeier et al., 2011a), and (b) the distribution of INA proteins over the droplet population can be described by a Poisson distribution, we developed the CHESS model (stoCHastic model of idEntical poiSSon distributed ice nuclei). In the model, it is assumed, that all INA protein complexes are identical and only the INA protein complexes initiate ice nucleation. Hence, the probability of freezing of a droplet containing one INA protein complex p_1 at temperature T according to Eq. (2) can be described as:

$$p_1 = 1 - \exp\left(-S_{\mathrm{site}} j_{\mathrm{het}}(T) t\right) \tag{7}$$

with the surface of an INA protein complex S_{site}, the temperature dependent heterogeneous ice nucleation rate coefficient j_{het}, and the ice nucleation time t. If a droplet possess $k > 1$ immersed INA protein complexes, the probability of freezing is increased due to a higher number of ice nucleation sites and therefore an increased ice nucleation active surface area kS_{site}. Following the assumption that all INA protein complexes have similar properties and hence identical surface areas, the probability of freezing of a droplet containing k INA protein complexes is given by:

$$p_k = 1 - \exp\left(-kS_{\mathrm{site}} j_{\mathrm{het}}(T) t\right) \tag{8}$$

ACPD
12, 21321–21353, 2012

Considering as next step a droplet ensemble containing Poisson distributed INA protein complexes at a certain temperature, the probability of droplet freezing is determined by the product of the probability that a droplet contains at least one INA protein complexe $P_\lambda(k \geq 1)$ and the probability p_k that this INA protein complex induce the immersion freezing:

$$f_{\text{ice}}(T) = \sum_{k=1}^{n} p_k P_\lambda(X = k). \tag{9}$$

After several conversion steps, we obtain the expression:

$$f_{\text{ice}}(T) = 1 - \exp(-\lambda(1 - \exp(-S_{\text{site}} j_{\text{het}}(T) t))). \tag{10}$$

Equation (10) describes the probability that one droplet out of a population, which contains on average λ INA protein complexes with an ice nucleating active surface S_{site} and a heterogeneous ice nucleation rate coefficient j_{het} of one single INA protein complex, freezes at temperature T after time t. All quantities of Eq. (10) are known except for S_{site} and j_{het}. Consequently, the product of these quantities, which corresponds to the heterogeneous ice nucleation rate $J_{\text{het}} = S_{\text{site}} j_{\text{het}}$ with the unit #/s, can be derived for a given ice nucleation time. The ice nucleation time t used for the calculation of J_{het} is defined as time period in which the temperature at the centerline of LACIS is in the range of $T_{\text{end}} + 0.3\,\text{K} \geq T \geq T_{\text{end}}$, whereby T_{end} depicts the temperature at the centerline at the outlet of LACIS. The results gained for 650 nm and 800 nm particles are shown in Fig. 7 (left panel) considering only the range in which the logarithm of the ice fraction increases linearly with temperature ($-7\,^\circ\text{C} \geq T \geq -10\,^\circ\text{C}$), i.e., the range in which the ice fraction is not influenced by the decreasing number of droplets available for freezing. J_{het} derived for both, 650 nm and 800 nm particles fall together within the level of uncertainty. In other words, as expected, the nucleation rate is no function of particle size or number of INA protein complexes. We should note again, that according to the derivation presented above, this is the nucleation rate for a single INA protein complex.

ACPD
12, 21321–21353, 2012

Now, we parameterize the ice nucleation rate J_{het} as function of temperature:

$$J_{het} = S_{site} j_{het}(T) = A \exp(B \cdot T) \quad (11)$$

with the coefficients $A = 1.55 \times 10^{-8}\,s^{-1}$ and $B = -2.032\,°C^{-1}$ being valid for INA protein complexes of *Pseudomonas syringae* bacteria. In general, A reflects kinetic effects and B thermodynamic effects of the ice nucleation.

As for the derivation of Eq. (10), the simplification of a time independent temperature was assumed, additional model simulations with Fluent/FPM were carried out in order to verify this simplification while the temperature change with time was accounted for. As a result, the coefficient B is not affected and the differences in coefficient A are less than 10 %. Hence the deviation is within the measuring uncertainty and can be neglected.

According to Cochet and Widehem (2000) (and references therein), the surface of an ice nucleating site of an INA protein structure can be assumed as a circular plane area with a diameter of 30 nm. So, we can determine the heterogeneous ice nucleation rate coefficient for a single INA protein complex j_{het}, which is depicted in Fig. 7 (right panel). j_{het} is a very steep function of temperature and increases from about $10^{13}\,\#/m^2s$ at −7 °C to $5 \cdot 10^{15}\,\#/m^2s$ at −10 °C. With these high values of j_{het} at relatively high temperatures, INA protein complexes from *Pseudomonas syringae* bacteria belong to the most active IN found.

In summary, the developed CHESS model, which accounts for the Poisson distribution of INA protein complexes over the considered droplet ensemble and follows the stochastic approach for describing the ice nucleation behavior of the identical INA protein complexes, has the advantage that the heterogenous ice nucleation rate/rate coefficient for a single INA protein complex can be derived from experimentally determined ice fractions in a very simple way if the average number of INA protein complexes per droplet is known.

It should be noted, that the CHESS model approach can generally be applied under the condition, that the IN are nearly identical concerning their ice nucleating properties

ACPD
12, 21321–21353, 2012

and Poisson distributed over the droplet population. This could be the case for, e.g. other biological particles such as pollen and spores.

4.4 Applicability of the CHESS model and comparison with other studies

In this chapter, the feasibility of the CHESS model for explaining the ice nucleation behavior of INA protein complexes from *Pseudomonas syringae* bacteria and the bacteria themself will be shown. This will be done using both, experimental data gained in the framework of the investigations at LACIS presented here, as well as data from earlier experiments (Möhler et al., 2008; Wood et al., 2002; Ward and DeMott, 1989; Yankofsky et al., 1981; Maki et al., 1974; Cochet and Widehem, 2000; Lindow et al., 1982; Maki and Willoughby, 1978). Results are shown in Fig. 8, depicting ice fractions as function of temperature for different experiments.

First, considering the results found at LACIS, the CHESS model (Eq. 10) accounting for the respective ice nucleation times reproduces the ice fractions measured (blue and black squares) for 650 nm ($\lambda = 0.228$, blue curve) and 800 nm ($\lambda = 0.536$, black curve) particles generated from a Snomax^{TM} solution/suspension, respectively, very well. Both, slope of the ice fraction curve, and ice fraction at saturation are nicely reproduced by the model. However, this is not surprising, as the model parameters (λ and J_{het}) were derived from this data. For the polydisperse measurements performed at LACIS (light blue square), λ has a value of 0.006 and the CHESS model (light blue line) predicts an increase of the ice fractions from 10^{-4} to its maximum value for temperatures ranging from −7.5 °C to −10 °C. The λ value for this polydisperse experiment is quite low because most of the particles generated from a Snomax^{TM} solution/suspension do not contain any or a small number of INA protein complexes initiating ice nucleation, as already shown in Fig. 6. This also holds for the study of Möhler et al. (2008) where the immersion freezing of polydisperse particles generated from a Snomax^{TM} solution/suspension was analyzed at −9.0 °C. For the determination of the ice fraction they assumed that the potential IN must have a certain size ($D_P \geq 600$ nm). But accounting for the fact that the INA protein complexes can be present at smaller

ACPD
12, 21321–21353, 2012

sizes, and calculating the ratio of measured number of IN per total number of particles given in the paper, the corrected ice fraction of the Möhler et al. (2008) study has a value of 0.009, which lies in the uncertainty range of the LACIS polydisperse measurement. In other words, utilizing the nucleation rate coefficient determined in the framework of this paper, we can with good accuracy predict the ice fraction found at LACIS and AIDA considering a polydisperse IN distribution.

Next, we apply the CHESS model to other experimental data. Therefore we use the above determined and parameterized heterogeneous ice nucleation rate (Eq. 11) which makes λ and the ice nucleation time t the only free parameters in the model, that have to be adjusted for reproducing the experimental data. Thus, we assume that in all considered experiments, ice nucleation is initiated by identical INA protein complexes featuring identical nucleation rates (Eq. 11). Under this assumption, varying λ and keeping t constant, an increase in λ, which corresponds to an increase of the number of INA protein complexes being present in the droplet population, will result in an increase of (a) the maximum ice fraction ($f^{\star}_{\mathrm{ice}}$), and (b) the temperature at which the ice fraction starts to rise. The latter results in a shift of the f_{ice} curve towards higher temperatures reflecting the fact that with increasing number of INA protein complexes being present, the probability of freezing increases, while the slope of f_{ice} does not change. By changing t and keeping λ constant, the ice fraction curves are shifted along the temperature axis, but again the slope of f_{ice} and also the maximum ice fraction is not affected. If λ is large enough, i.e. $f^{\star}_{\mathrm{ice}}$ is equal to one, increasing λ or t will both result in a shift of the f_{ice} curve towards higher temperatures. In fact, in this range, there is a relation between λ and t implying that when analyzing experimental data with the CHESS model, with increasing t, λ will decrease and vice versa. This allows for analyzing experimental data even if the exact nucleation time is unknown as is the case for the investigations presented below. Therefore, in the following considerations an ice nucleation time of 1 s can be assumed for convenience.

We start with ice fractions determined in the study of Wood et al. (2002) (green diamonds), in which the immersion freezing of freely falling droplets containing parti-

ACPD
12, 21321–21353, 2012

cles from a Snomax^{TM} solution/suspension filtrate smaller than 200 nm was analyzed. By the means of the CHESS model an average number of INA protein complexes of approx. 5.9 (green line) is calculated. The slopes of the measured and predicted f_{ice} curves agree very well. From this it follows that in Wood et al. (2002) a temperature dependence of the heterogeneous ice nucleation rate similar to that in our study was found.

Ward and DeMott (1989) (not shown in Fig. 8) studied the immersion freezing of highly concentrated (10^{12}–10^{13} nuclei per gram) Snomax^{TM} solution/suspension droplets and determined freezing temperatures between approx. 0 °C and −5 °C. The shift to higher temperatures is consistent with the CHESS model for the high λ values which reflects the high numbers of INA protein complexes being present in the droplets investigated.

Interestingly, the CHESS model is able to reproduce the ice nucleation behavior of bacteria as well. This can be seen when comparing results given in Yankofsky et al. (1981) (dark brown dots), analyzing the freezing of droplets with multiple immersed *Pseudomonas syringae* bacteria cells, with results from the CHESS model (dark brown line). The slopes of measured and calculated ice fraction curves also agree with a reasonably small deviation. In this case the CHESS model predicts an average number of INA protein complexes of 31.1.

Considering another study dealing with immersion freezing of droplets containing multiple *Pseudomonas syringae* bacteria cells (red dots) performed by Maki et al. (1974), the CHESS model reproduces the experimental findings in terms of temperature dependence and average number of INA protein complexes, however, with slightly larger deviations. In order to reproduce the experimentally determined ice fractions from Maki et al. (1974) the λ value has to be in a range of 10^4–10^5 (orange and red line), which is in line with the cell concentration of 10^4 cells per droplet given in the paper. However, the latter finding might be simply coincidence, as we do not know the exact nucleation times considered in the experiment.

ACPD
12, 21321–21353, 2012

The shift of the ice fraction curves to higher freezing temperatures with increasing number of bacteria cells was found in several studies. In Cochet and Widehem (2000) it was found, that a higher cell concentration of *Pseudomonas syringae* bacteria leads to higher freezing temperatures. Furthermore, Lindow et al. (1982) recognized a shift to lower temperatures with decreasing number of bacteria cells per droplet. Analyzing the freezing behavior of a droplet population with low cell concentrations Maki and Willoughby (1978) also figured out, that not all the droplets froze although the temperature was sufficiently low. This can be explained by the fact that not all droplets contained a bacteria cell acting as IN, which is consistent with our findings.

Summarizing the results shown above, it can be stated that the CHESS model is capable of modeling both, the ice nucleation behavior of freely existing INA protein complexes and complexes attached to the outer membrane of bacteria cells, based on the heterogeneous ice nucleation rate coefficient of the single INA protein complex. In other words, (a) the temperature range in which heterogeneous droplet freezing occurs, and the fraction of droplets being able to freeze, depend on the actual number of INA protein complexes being present in the droplet ensemble, and (b) the temperature dependence of the heterogeneous ice nucleation rate and rate coefficient is the same regardless of the actual state of the INA protein complex (free or attached). It should be noted that the CHESS model in principle can be applied to all scenarios, in which heterogeneous ice nucleation is controlled by identical ice nucleating sites being Poisson distributed over a droplet population.

5 Summary and conclusion

At LACIS, the immersion freezing behavior of INA protein complexes produced from a Snomax^{TM} solution/suspension was investigated as function of temperature in a range of −5 °C to −38 °C. We found that INA protein complexes controlling the ice nucleation behavior of *Pseudomonas syringae* bacteria belong to the most active IN

ACPD
12, 21321–21353, 2012

considered up to now. It was observed that the ice fraction increases almost linearly between −7 °C and −10 °C and levels off at lower temperatures, i.e., exhibits a saturation behavior. Assuming that immersion freezing is initiated by INA protein complexes, we conclude first that only one class of INA protein complexes is present in the particles/droplets, most likely the class C protein complex. Second not all droplets contain an INA protein complex and the number of INA protein complexes varies between different particles, more precisely, it is Poisson distributed over a monodisperse particle population. Applying the Poisson distribution, the average number of INA protein complexes, per particle and, as each droplet in LACIS contains only a single particle, consequently per droplet can be determined. Additionally, investigating different sizes of particles generated from a Snomax™ solution/suspension, meaning different average numbers of INA protein complexes λ, it was found that λ is a function of particle volume. Knowing λ as function of particle volume, the IN size distribution can be determined and showing that the number of INA increases with particle size. In fact, even 100 nm particles generated from a Snomax™ solution/suspension contain INA protein complexes which is in contradiction to earlier studies by Möhler et al. (2008) who assumed only particles larger than 600 nm to be ice active. It should be noted, that a determination of λ is only possible if the maximal ice fraction is below 1. From this it follows that immersion freezing studies of droplet ensembles with small numbers of INA protein complexes immersed in the droplets are advantageous, as only this way the heterogeneous ice nucleation rate/rate coefficient for a single INA protein complex can be properly determined.

In order to derive the heterogeneous ice nucleation rate/rate coefficient of one single INA protein complex a simple model, the CHESS model (stoCHastic model of idEntical poiSSon distributed ice nuclei), was developed. The CHESS model combines the assumptions that the INA protein complexes are Poisson distributed over the droplet ensemble and that the heterogeneous ice nucleation on identical INA protein complexes is a stochastic process. Under these assumptions, the heterogeneous ice nucleation rate of a single INA protein complex was parameterized as function of temperature.

ACPD
12, 21321–21353, 2012

Assuming a circular plane area with a diameter of 30 nm for the surface of the INA protein complexes, the heterogeneous ice nucleation rate coefficient was found to be a very steep function of temperature, increasing from about 10^{13} #/m^{2}s at −7 °C to 5×10^{15} #/m^{2}s at −10 °C.

Additionally, with use of the CHESS model, experimental results from earlier experiments considering the immersion freezing behavior of *Pseudomonas syringae* bacteria and the related INA protein complexes were analyzed. Comparing results of these studies, the average number of INA protein complexes was found to vary over several orders of magnitude affecting the actual temperature range in which freezing was observed. Applying the temperature dependent heterogeneous ice nucleation rate for one single INA protein complex determined in our study, we found consistently good agreement with the results presented in e.g. Wood et al. (2002) and Yankofsky et al. (1981). In other words, the CHESS model, together with the the heterogeneous nucleation rate of the single INA protein complexes, can consistently explain the immersion freezing behavior of both, freely exiting INA protein complexes and complexes attached in the outer membrane of bacteria cells.

Finally, we note that application of the CHESS model improved our basic understanding of immersion freezing induced by INA protein complexes. However, application of the CHESS model is most likely not limited to INA protein complexes only. In fact, it could be applied for other IN types, e.g. ice active protein complexes from other bacteria or macro-molecules from pollen (Pummer et al., 2012), under the condition that the specific IN's ice nucleation properties are nearly identical and the IN are Poisson distributed over the droplet population. Consequently, it could prove highly useful for modeling the immersion freezing behavior of biological particles such as bacteria and pollen in e.g. cloud-microphysics resolving models.

Acknowledgements. This research project was partly funded by the German Research Foundation (DFG project WE 4711/1-1) research unit INUIT.

ACPD
12, 21321–21353, 2012

References

Ansmann, A., Tesche, M., Seifert, P., Althausen, D., Engelmann, R., Fruntke, J., Wandinger, U., Mattis, I., and Müller, D.: Evolution of the ice phase in tropical altocumulus: SAMUM lidar observations over Cape Verde, J. Geophys. Res.-Atmos., 114, 20 pp., 17208, doi:10.1029/2008JD011659, 2009. 21323

Clauss, T., Kiselev, A., Hartmann, S., Augustin, S., Pfeifer, S., Niedermeier, D., Wex, H., and Stratmann, F.: Application of linear polarized light for the discrimination of frozen and liquid droplets in ice nucleation experiments, submitted to Atmos. Meas. Tech. Discuss., 2012. 21327

Cochet, N. and Widehem, P.: Ice crystallization by Pseudomonas syringae, Appl. Microbiol. Biot., 54, 153–161, doi:10.1007/s002530000377, 2000. 21323, 21324, 21335, 21336, 21339

Green, R. L. and Warren, G. J.: Physical and functional repetition in an bacterial ice nucleation gene, Nature, 317, 645–648, 1985.

Govindarajan, A. G. and Lindow, S. E.: Size of bacterial ice-nucleation sites measured in-situ by radiation inactivation analysis, P. Natl. Acad. Sci. USA, 85, 1334–1338, 1988.

Hartmann, S., Niedermeier, D., Voigtländer, J., Clauss, T., Shaw, R. A., Wex, H., Kiselev, A., and Stratmann, F.: Homogeneous and heterogeneous ice nucleation at LACIS: operating principle and theoretical studies, Atmos. Chem. Phys., 11, 1753–1767, doi:10.5194/acp-11-1753-2011, 2011. 21325, 21326, 21327, 21328

Kamphus, M., Ettner-Mahl, M., Klimach, T., Drewnick, F., Keller, L., Cziczo, D. J., Mertes, S., Borrmann, S., and Curtius, J.: Chemical composition of ambient aerosol, ice residues and cloud droplet residues in mixed-phase clouds: single particle analysis during the Cloud and Aerosol Characterization Experiment (CLACE 6), Atmos. Chem. Phys., 10, 8077–8095, doi:10.5194/acp-10-8077-2010, 2010. 21323

Knutson, E. O. and Whitby, K. T.: Aerosol classification by electric mobility: apparatus, theory and applications, J. Aerosol Sci., 6, 443–451, 1975. 21326

Levin, Z. and Yankofsky, S. A.: Contact versus immersion freezing Of freely suspended droplets by bacterial ice nuclei, J. Clim. Appl. Meteorol., 22, 1964–1966, 1983. 21323, 21324

Lindow, S. E., Arny, D. C., and Upper, C. D.: Bacterial ice nucleation – a factor in frost injury to plants, Plant Physiol., 70, 1084–1089, 1982. 21324, 21336, 21339

Maki, L. R. and Willoughby, K. J.: Bacteria as biogenic sources of freezing nuclei, J. Appl. Meteorol., 17, 1049–1053, 1978. 21324, 21336, 21339

ACPD
12, 21321–21353, 2012

Maki, L. R., Galyan, E. L., Chang-Chien, M.-M., and Caldwell, D. R.: Ice nucleation induced by pseudomonas-syringae, Appl. Microbiol., 28, 456–459, 1974. 21323, 21324, 21336, 21338

Möhler, O., Georgakopoulos, D. G., Morris, C. E., Benz, S., Ebert, V., Hunsmann, S., Saathoff, H., Schnaiter, M., and Wagner, R.: Heterogeneous ice nucleation activity of bacteria: new laboratory experiments at simulated cloud conditions, Biogeoscience, 5, 1425–1435, doi:10.5194/bg-5-1425-2008, 2008. 21323, 21324, 21332, 21336, 21337, 21340

Niedermeier, D., Hartmann, S., Shaw, R. A., Covert, D., Mentel, T. F., Schneider, J., Poulain, L., Reitz, P., Spindler, C., Clauss, T., Kiselev, A., Hallbauer, E., Wex, H., Mildenberger, K., and Stratmann, F.: Heterogeneous freezing of droplets with immersed mineral dust particles – measurements and parameterization, Atmos. Chem. Phys., 10, 3601–3614, doi:10.5194/acp-10-3601-2010, 2010. 21326, 21327

Niedermeier, D., Shaw, R. A., Hartmann, S., Wex, H., Clauss, T., Voigtländer, J., and Stratmann, F.: Heterogeneous ice nucleation: exploring the transition from stochastic to singular freezing behavior, Atmos. Chem. Phys., 11, 8767–8775, doi:10.5194/acp-11-8767-2011, 2011a. 21325, 21333

Niedermeier, D., Hartmann, S., Clauss, T., Wex, H., Kiselev, A., Sullivan, R. C., DeMott, P. J., Petters, M. D., Reitz, P., Schneider, J., Mikhailov, E., Sierau, B., Stetzer, O., Reimann, B., Bundke, U., Shaw, R. A., Buchholz, A., Mentel, T. F., and Stratmann, F.: Experimental study of the role of physicochemical surface processing on the IN ability of mineral dust particles, Atmos. Chem. Phys., 11, 11131–11144, doi:10.5194/acp-11-11131-2011, 2011b. 21326, 21327

Pratt, K. A., DeMott, P. J., French, J. R., Wang, Z., Westphal, D. L., Heymsfield, A. J., Twohy, C. H., Prenni, A. J., and Prather, K. A.: In situ detection of biological particles in cloud ice-crystals, Nat. Geosci., 2, 397–400, doi:10.1038/ngeo521, 2009. 21323

Pruppacher, H. R. and Klett, J. D.: Microphysics of Clouds and Precipitation, Kluwer Academic Publishers, Dordrecht, The Netherlands, 13 pp., 1997. 21325

Pummer, B. G., Bauer, H., Bernardi, J., Bleicher, S., and Grothe, H.: Suspendable macromolecules are responsible for ice nucleation activity of birch and conifer pollen, Atmos. Chem. Phys., 12, 2541–2550, doi:10.5194/acp-12-2541-2012, 2012. 21341

Seifert, P., Ansmann, A., Mattis, I., Wandinger, U., Tesche, M., Engelmann, R., Müller, D., Pérez, C., and Haustein, K.: Saharan dust and heterogeneous ice formation: eleven years of cloud observations at a Central European EARLINET site, J. Geophys. Res.-Atmos., 115, 20201, doi:10.1029/2009JD013222, 2010. 21323

ACPD
12, 21321–21353, 2012

Southworth, M. W., Wolber, P. K., and Warren, G. J.: Nonlinear relationship between concentration and activity of a bacterial ice nucleation protein, J. Biol. Chem., 263, 15211–15216, 1988. 21323

Stratmann, F., Kiselev, A., Wurzler, S., Wendisch, M., Heintzenberg, J., Charlson, R. J., Diehl, K., Wex, H., and Schmidt, S.: Laboratory studies and numerical simulations of cloud droplet formation under realistic supersaturation conditions, J. Atmos. Ocean. Tech., 21, 876–887, 2004. 21325, 21326

Turner, M. A., Arellano, F., and Kozloff, L. M.: Three separate classes of bacterial ice nucleation structures, J. Bacteriol., 172, 2521–2526, 1990. 21323, 21324, 21329, 21330

Turner, M. A., Arellano, F., and Kozloff, L. M.: Components of ice nucleation structures of bacteria, J. Bacteriol., 173, 6515–6527, 1991. 21323, 21329

Twohy, C. H. and Poellot, M. R.: Chemical characteristics of ice residual nuclei in anvil cirrus clouds: evidence for homogeneous and heterogeneous ice formation, Atmos. Chem. Phys., 5, 2289–2297, doi:10.5194/acp-5-2289-2005, 2005. 21323

Vali, G.: Quantitative evaluation of experimental results on heterogeneous freezing nucleation of supercooled liquids. J. Atmos. Sci., 28, 402–409, 1971. 21331

Vali, G., Christensen, M., Fresh, R. W., Galyan, E. L., Maki, L. R., and Schnell, R. C.: Biogenic ice nuclei. Part II: Bacterial sources. J. Atmos. Sci., 33, 1565–1570, 1976. 21323, 21324

Ward, P. J. and DeMott, P. J.: Preliminary experimental evaluation of Snomax^{TM} snow inducer, *pseudomonas syringae*, as an artificial ice nucleus, J. Weather Mod., 21, 9–13, 1989. 21323, 21336, 21338

Warren, G. J. and Wolber, P. K.: Heterogeneous ice nucleation by bacteria, Cryo Lett., 8, 204–217, 1987. 21323

Wilck, M., Stratmann, F., and Whitby, E.: A fine particle model for fluent: description and application, in: Proc. Sixth Int. Aerosol Conf., Chinese Association for Aerosol Research in Taiwan/International Aerosol Research Assembly, Taipei, Taiwan, 1269–1270, 2002. 21328

Wolber, P. K. and Warren, G. J.: Bacterial ice-nucleation proteins, Trends Biochem. Sci., 14, 179–182, 1989. 21323

Wood, S. E., Baker, M. B., and Swanson, B. D.: Instrument for studies of homogeneous and heterogeneous ice nucleation in free-falling supercooled water droplets, Rev. Sci. Instrum., 73, 3988–3996, 2002. 21324, 21332, 21336, 21337, 21338, 21341

ACPD
12, 21321–21353, 2012

Yankofsky, S. A., Levin, Z., Bertold, T., and Sandlerman, N.: Some basic characteristics of bacterial freezing nuclei, J. Appl. Meteorol., 20, 1013–1019, 1981. 21323, 21324, 21331, 21336, 21338, 21341

ACPD
12, 21321–21353, 2012

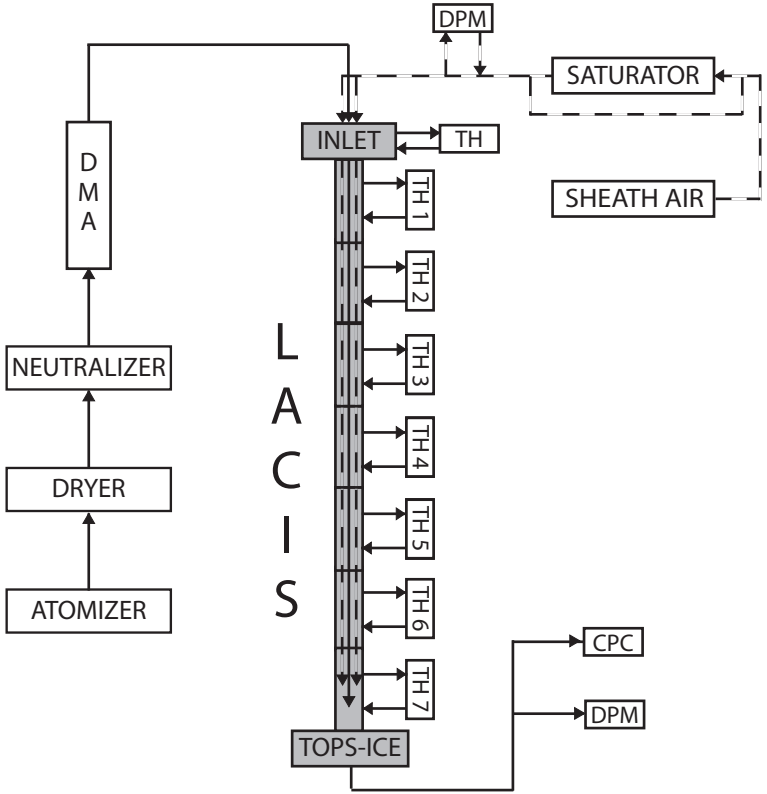

Fig. 1. Setup of the particle generation, the LACIS flow tube and optical detection system. The abbreviation DMA depicts Differential Mobility Analyzer, DPM represents chilled mirror dew point hygrometer, TH means thermostat, TOPS-ICE declares Thermally Stabilized Optical Particle Spectrometer and CPC depicts the condensational particle counter.

ACPD
12, 21321–21353, 2012

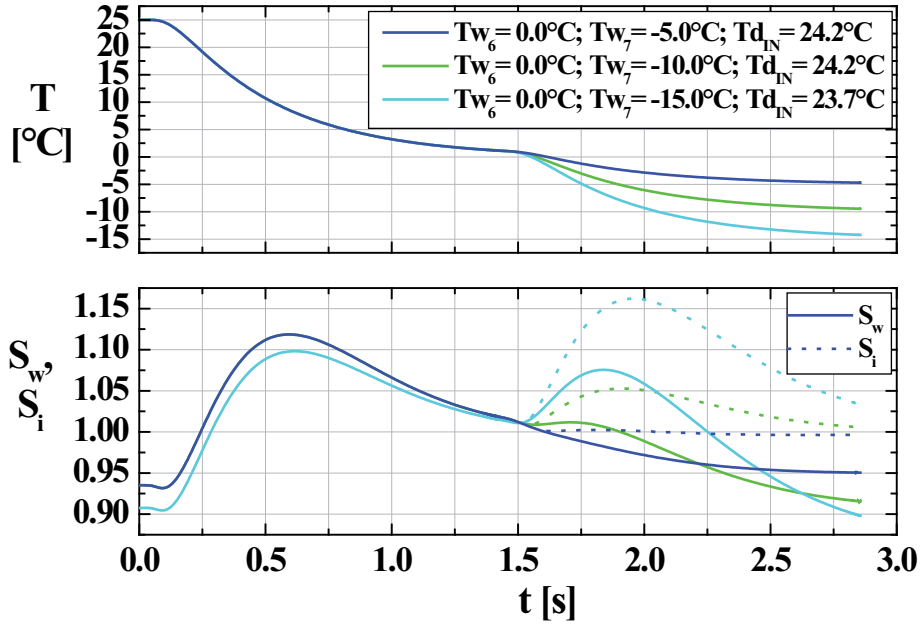

Fig. 2. Temperature T (upper panel) and saturation wrt. water S_w (solid lines, the lower panel) and ice S_i (dotted lines, the lower panel) as function of residence time t of sections 6 and 7 for different boundary conditions (with wall temperature T_w and inlet dew point temperature T_{dIN}).

ACPD
12, 21321–21353, 2012

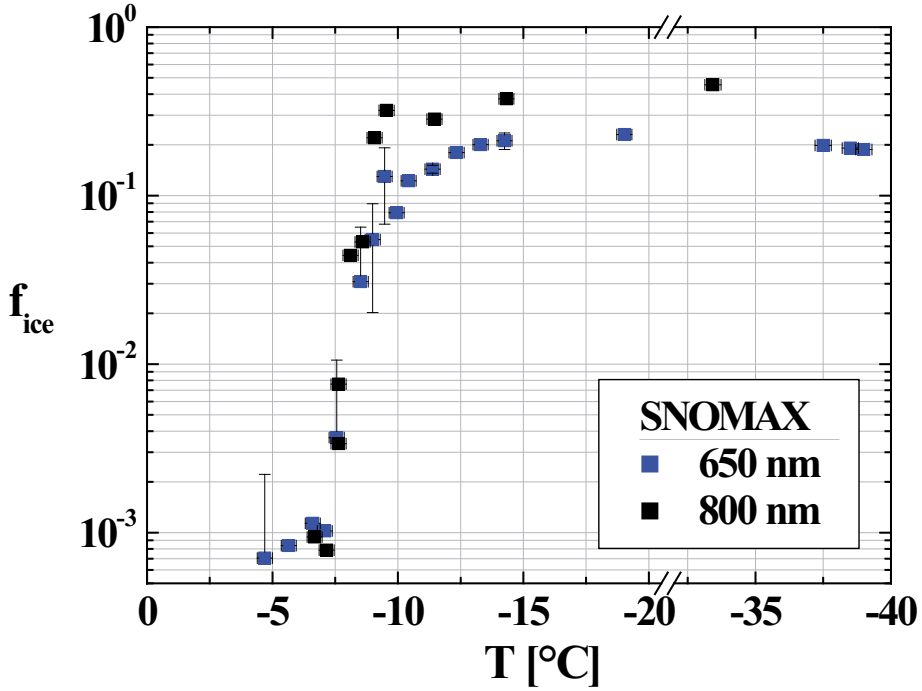

Fig. 3. Ice fraction f_{ice} as function of temperature T for 650 nm and 800 nm particles generated from a Snomax^{TM} solution/suspension.

ACPD
12, 21321–21353, 2012

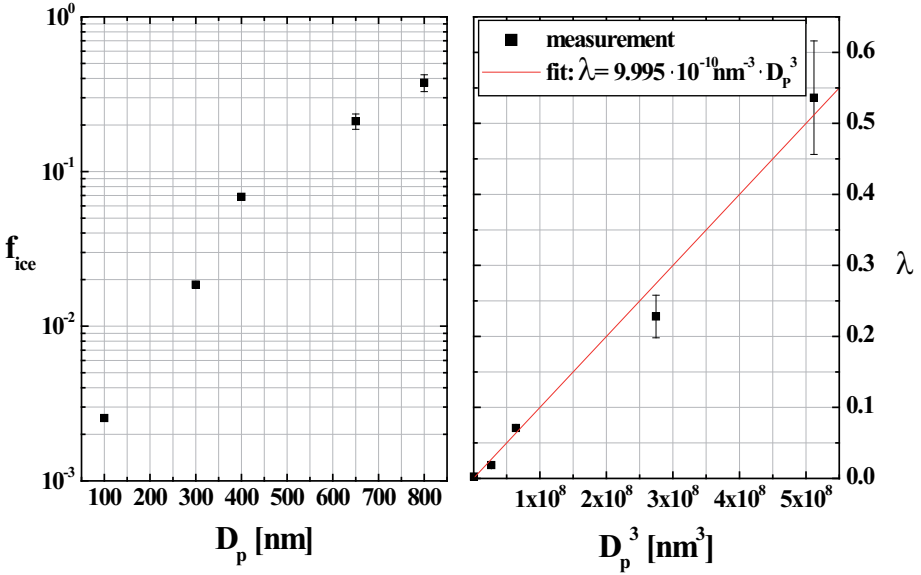

Fig. 4. Ice fraction f_{ice} vs. mobility diameter D_p (left panel) at $T = -15\,^{\circ}C$ (saturation range). Measured λ and fit function of λ, describes the average number of INA protein complexes per particle generated from a Snomax^{TM} solution/suspension, as function of particle volume (D_P^3) (right panel).

ACPD
12, 21321–21353, 2012

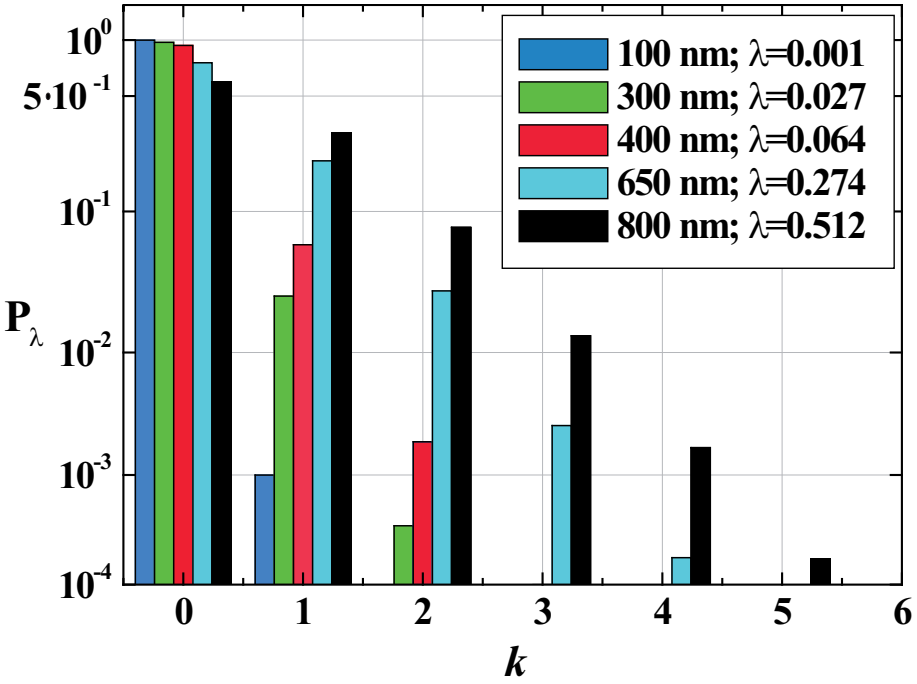

Fig. 5. Probability P_λ of occurring $k = 0, 1, 2, 3, 4, 5$ INA protein complexes per droplet (Poisson distributed) for different average numbers of INA protein complexes λ (corresponds to different mobility diameters of particles generated from a Snomax^{TM} solution/suspension) is shown.

ACPD
12, 21321–21353, 2012

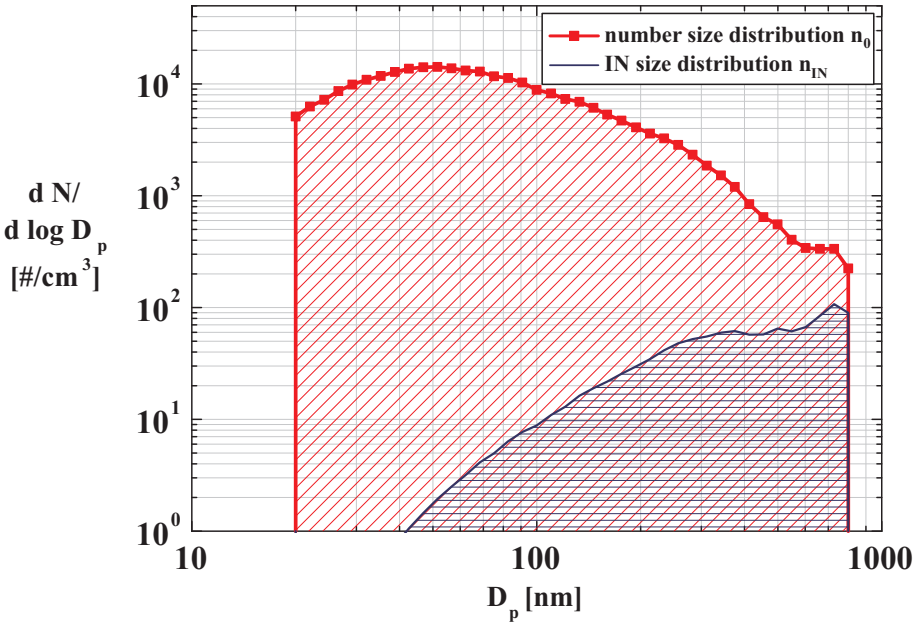

Fig. 6. Number size distribution of particles generated from a Snomax^{TM} solution/suspension n_0 and derived IN size distribution n_{IN} containing INA protein complexes.

ACPD
12, 21321–21353, 2012

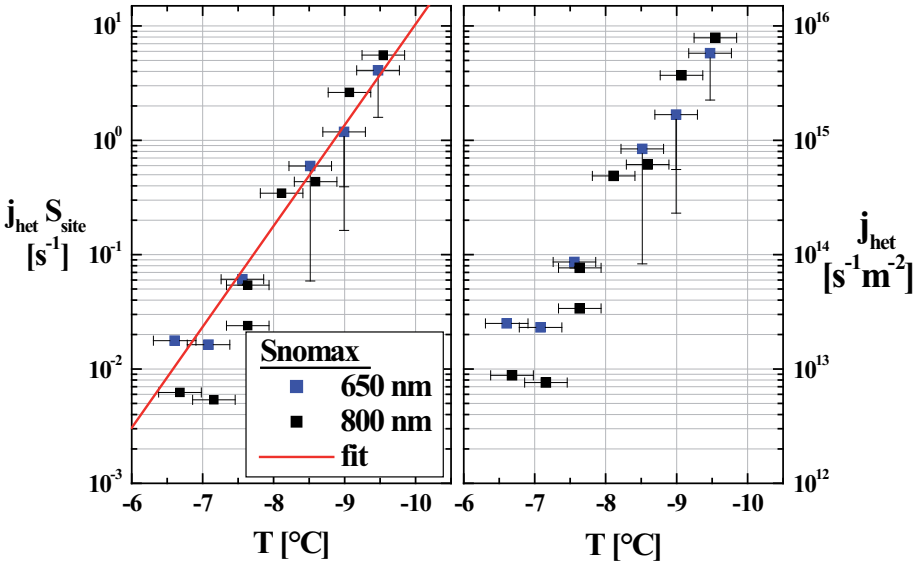

Fig. 7. Heterogeneous ice nucleation rate ($J_{het} = j_{het}S_{site}$) as function of temperature T (left panel) and rate coefficient j_{het} assuming $S_{site} = \pi(15\ \text{nm})^2$ derived from 650 nm and 800 nm particles generated from a Snomax™ solution/suspension. Both quantities represent ice nucleation behavior of one single INA protein complex.

ACPD
12, 21321–21353, 2012

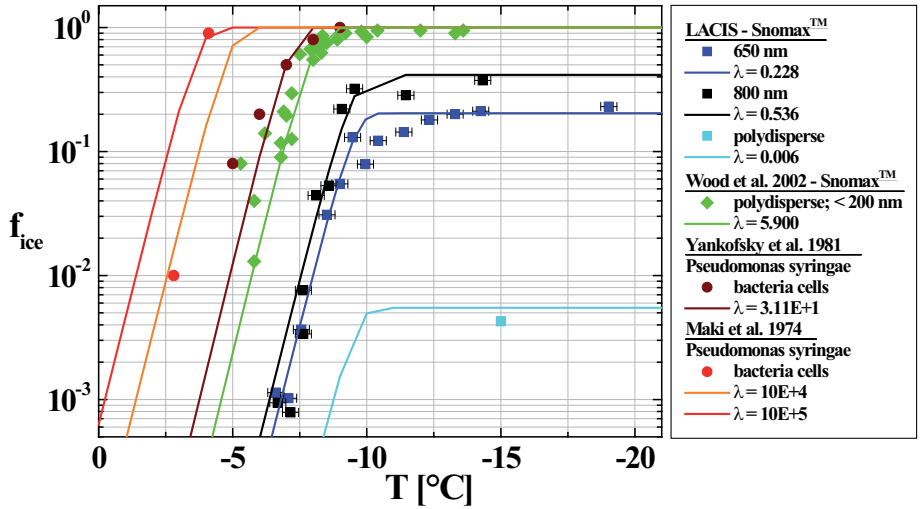

Fig. 8. A comparison of measured and calculated ice fractions obtained from the CHESS model with data from literature, see legend. Measured (data points) and calculated (lines) ice fractions f_{ice} are given as function of temperature T.

ACPD
12, 21321–21353, 2012